ARTICLE

Check for updates

Deforestation and climate change are projected to increase heat stress risk in the Brazilian Amazon

Beatriz Fátima Alves de Oliveira [1✉], Marcus J. Bottino[2], Paulo Nobre[2] & Carlos A. Nobre[3]

Land use change and deforestation can influence local temperature and climate. Here we use a coupled ocean-atmosphere model to assess the impact of savannization of the Amazon Basin on the wet-bulb globe temperature heat stress index under two climate change scenarios (RCP4.5 and RCP8.5). We find that heat stress exposure due to deforestation was comparable to the effect of climate change under RCP8.5. Our findings suggest that heat stress index could exceed the human adaptation limit by 2100 under the combined effects of Amazon savannization and climate change. Moreover, we find that risk of heat stress exposure was highest in Northern Brazil and among the most socially vulnerable. We suggest that by 2100, savannization of the Amazon will lead to more than 11 million people will be exposed heat stress that poses an extreme risk to human health under a high emission scenario.

[1] Fiocruz Regional Office of Piauí, National School of Public Health, Oswaldo Cruz Foundation, Teresina, Piauí, Brazil. [2] National Institute for Space Research - INPE, Cachoeira Paulista, São Paulo, Brazil. [3] Institute of Advanced Studies (IEA), São Paulo University, São Paulo, São Paulo, Brazil.
✉email: beatrizenf@gmail.com

Global warming is causing heat stress conditions that are becoming more frequent and intense in many tropical and subtropical regions of the world[1,2]. In 2020, the warmest September in history was recorded, with several locations in Europe and South America breaking record-high temperatures[3], while the high temperatures in Midwestern and Northern Brazil posed a risk for death by hyperthermia[4]. A recent study found that these two regions have the largest projected air temperature changes driven by a global warming scenario in the Eta atmospheric regional model nested in global climate models (HadGEM-ES and MIROC)[5].

The recent extreme heat exposure in Brazil occurred during a period marked by forest fires and growing deforestation rates in several biomes, especially in the Brazilian Amazon[6,7]. Between August 2019 and July 2020, total deforestation in the Brazilian Amazon experienced the single highest year-to-year increase since 2010 (nearly 1000 km²)[6]. Increased deforestation is an important sign of non-compliance with the goals established by the 2015 Paris Agreement (which were intended to limit global warming to 1.5–2.0 °C). To achieve this established goal, greenhouse gas emissions should reach zero by 2050 in industrialized countries and by 2100 in the rest of the world, assuming that natural carbon sinks are preserved, which has not been observed in recent years. The deforested area reached in 2020 is much larger than the commitment specified in Brazil's National Policy[8], which sought an 80% decrease in deforestation in the Amazon compared with the average verified deforestation levels from 1996 and 2005. That is, the target deforestation rate in 2020 should be 3925 km² instead of the actual 2020 rate of 11,022 km².

The Amazon rainforest is one of the most biodiverse regions in the world[9,10], and its progressive deforestation may result in abrupt and profound changes in the regional climate and intensification of extreme climate events[11,12]. Nobre et al.[13] predicted a nearly 60% rainfall reduction and a 2 °C increase in the near-surface air temperature over the Amazon based on a scenario of Amazonian deforestation incorporating ocean–atmosphere coupling. Such profound climatic changes over the Amazon along with large-scale projected deforestation scenarios will aggravate the effects of heat exposure on human adaptation, work activities, leisure, and sports practice[14], especially for vulnerable social groups. In this study, we carried out numerical climate modeling experiments using the Brazilian Earth System Model (BESM-2.5)[15–17] to assess the effects of two major climate stressors, i.e., Amazon savannization and global climate change, on the risk of exposure to heat stress conditions with respect to the potential impact on human health.

Excessive heat-related morbidity and mortality are linked to the body's ability to maintain a stable internal temperature[18]. Under unfavorable environmental conditions that include high temperature and humidity exposure, the body's cooling capabilities are weakened, resulting in increased body temperature. Sustained exposure to such conditions results in dehydration and exhaustion, and in more severe cases, tension and collapse of vital functions, which can lead to death[19]. In addition, heat stress affects mood and mental illness and reduces physical and psychological performance[20].

Increased body temperature due to heat stress is an unbalanced condition in which heat production or gain outpaces heat loss. This condition depends on interactions between at least four climatic variables: air temperature, relative humidity, solar radiation, and wind speed. In environments with air temperatures above 35 °C, transpiration/evaporation is the body's main cooling process; in environments with high humidity (and low wind speeds), this mechanism is less effective and the body's heat balance can be compromised. Outside of environmental factors, clothing, physical activity, and acclimatization can also affect heat stress[21,22].

There are various heat exposure stress indices that can be measured, including rational indices (via calculations involving heat balance equation), empirical indices (based on objective and subjective strain), and direct indices (involving direct measurement of environmental variables)[19]. Direct indices are more applicable, as these indices are based on monitoring environmental variables. Among these indices, the wet-bulb globe temperature (WBGT) is the most used, especially in military training, work safety, sports medicine, and leisure activities[22–24].

The WBGT heat index incorporates the natural wet-bulb temperature (Tnwb), the black globe temperature (Tg), and air temperature (Ta), which can be calculated using standard meteorological observations (temperature, humidity, wind speed, and solar radiation) for both in-shade environments (without solar radiation exposure) and outdoor environments (with solar radiation exposure). This index is properly adjusted for actions in work environments based on various metabolic rates defined in international[22] and national[25,26] standards, which recommend an hourly rest period during heavy work when the WBGT exceeds 26 °C and suspension of work activities when the WBGT reaches 34 °C. Under more extreme conditions, e.g., a WBGT >40 °C, exposure may compromise survivability in heat-vulnerable groups[2,27].

Results and discussion

Amazon savannization and heat stress. The results of our Amazon Basin savannization simulations, which examined the worst-case scenario, i.e., that the entire Amazon rainforest is replaced with savannah, revealed increased air temperatures and decreased relative humidity and precipitation, especially in the Amazon Basin (Supplementary Figs. 1–3). Such climatic conditions were enhanced when the savannization experiments were computed in tandem with the atmospheric radiative forcing of the representative concentration pathways (RCP) 4.5 and 8.5 (Supplementary Fig. 1). The various model experiments were explicitly named using the following legend: greenhouse gas scenario (H – Historical, 45 – Representative Concentration Pathways 4.5 – RCP4.5, and Representative Concentration Pathways 85 – RCP8.5); and land-use scenarios (F – Forested, S – Savannah). For instance, HS represents the historical greenhouse gas scenario with the savannah land use pattern and 85F indicates the RCP8.5 greenhouse gas scenario run with the forested land use pattern.

Regarding heat stress conditions, computation of the WBGT index for these simulations revealed the most dramatic effects of Amazon savannization on the regional scale. In the hottest month, the average daily maximum in-shade WBGT values exceeded the limit associated with the extreme risk to human health (i.e., WBGT ≥ 34 °C), reaching maxima of 37 and 41 °C for the 45S and 85S simulations, respectively (Fig. 1). The distribution of in-shade WBGT values showed that a large majority of the Amazon Basin region reached 34 °C, with some areas reaching 41 °C in the 85 S simulation. Such high WBGT values were not obtained in forested simulations, even under the most extreme 85F simulation (Fig. 1). For outdoor conditions, the maximum daily average of the WBGT in the hottest month reached 46 °C for the 85S simulation (Supplementary Fig. 4).

In a simulation under historical atmospheric conditions (i.e., the present conditions), Amazon savannization led to 1–5 °C increases in the average daily highest in-shade WBGT values during the hottest month over the Amazon (Fig. 1, difference of HS − HF). In the climate change scenarios, the increase in WBGT reached 7.5 °C with more robust effects in the RCP8.5 scenario (Fig. 1; difference of 85S − 85F). On the regional scale, deforestation also increased the average values of
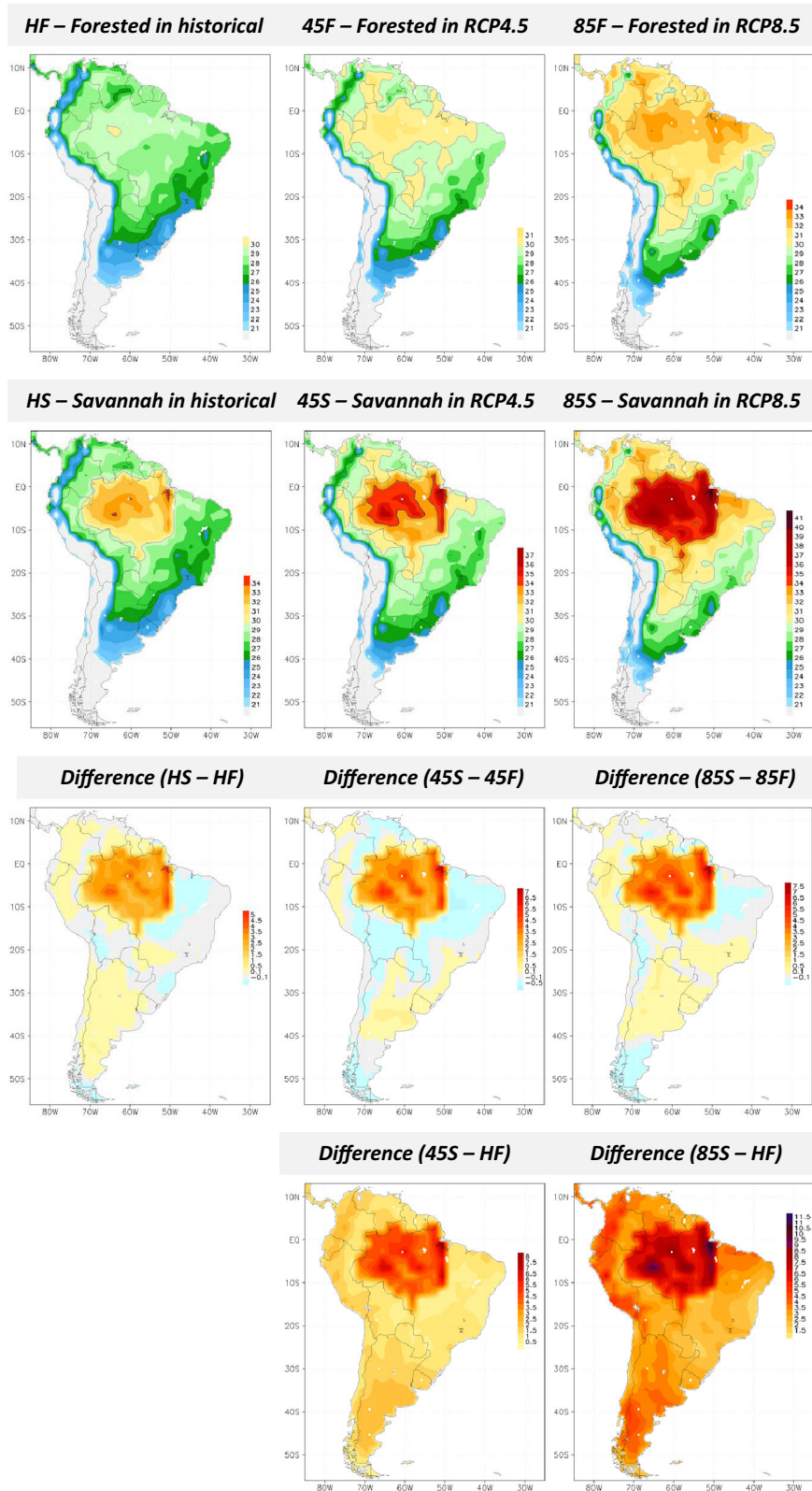
Fig. 1 Average daily maxima of the in-shade WBGT (in °C) for the warmest months. Average daily maxima of the in-shade WBGT (in °C) for the warmest months according to global climate change scenarios for the historical (1980–2010) and RCP4.5 and RCP8.5 (2073–2100) periods, and land-use scenarios. Global warming scenarios (Historical – H, RCP4.5 – 45, RCP8.5 – 85) and land-use scenarios (Forested – F and Savannah – S).

the daily maximum in-shade WBGT by 0.5 °C over the Andean and South and Southeastern Brazilian regions in the RCP8.5 scenario (Fig. 1; difference of 85S − 85F).

The combined effects of the deforestation and global warming scenarios contributed to extreme levels of in-shade WBGT heat stress risk in most of the Amazon region, showing an increase of up to 11.5 °C under the RCP8.5 scenario (Fig. 1, difference of 85S − HF) by the end of the twenty-first century relative to the present conditions, as shown in Fig. 1. On the regional scale for most of South America (except for the Amazon Basin region), the average maximum daily in-shade WBGT values were projected to increase by 2–5.5 °C during the hottest months for 2073–2100 compared with the historical period without deforestation. Similar effects were observed for the outdoor conditions (Supplementary Fig. 4).

Regarding the effects on human health, elevated heat stress exposure due to deforestation could be extremely dangerous to humans, including increased risk of intolerable conditions for in-shade working activities[23] and intensified risk of heat-related illness[28]. Furthermore, increased heat stress exposure might increase morbidity and mortality in heat-vulnerable populations, including children, the elderly, and those with underlying health conditions[29,30].

Figure 2 shows histograms of the distributions of the daily maximum in-shade and outdoor WBGT values, highlighting the heat stress exposure risk thresholds (dashed lines), as influenced by savannization and the climate change scenarios in the Amazon Basin. The data show that under in-shade conditions, replacement of the current forest cover with savanna-type vegetation during the baseline/historical period could lead to a daily maximum WBGT distribution equivalent to that predicted by the RCP8.5 climate scenario at the end of the century. Thus, Amazon rainforest deforestation has a local effect on heat stress exposure equivalent to that of the most severe effect of climate change, magnifying the frequency and intensity of extreme in-shade WBGT values. The distribution of the maximum daily

in-shade WBGT values shows a shift in the warming values for the RCP4.5 and RCP8.5 scenarios, with the most frequent values near 32 °C for 45S and 34 °C 85S simulations. In the latter scenario, this means that the daily maximum in-shade WBGT might exceed 34 °C on 42% of the days in each year at the end of this century.

In outdoor environments, the most notable effects of savannization and climate change are on the threshold of survivability. Under the 85 S simulation, the distribution of the daily maximum WBGT values reached values greater than 40 °C on 7% of days (i.e., 25 days per year) at the end of this century in the Amazon Basin region (Fig. 2). On some days, the WBGT exceeded the daily maximum value of 46 °C, highlighting the alarming possibility of deadly heat stress levels resulting from the combined effects of deforestation and climate change. Although climatic models, including the BESM model used here, present uncertainties in their projections, our findings suggest that the limits of human adaptation could be exceeded in this region if current trends in Amazon rainforest deforestation and global climate change continue to increase. In the 85S simulation, it would be impossible to perform heavy outdoor activities for at least 1 h/day[22] in 42% of the days studied (relative to WBGT ≥ 34 °C). If this scenario occurs, new occupational health initiatives, preventive measures, and shifts to safer behaviors will be required to reduce the impact of heat stress exposure.

In the context of human health impact, the combined effects of global climate change and Amazon rainforest savannization could represent an exposure of more than six million people to conditions of extreme risk to human health (WBGT ≥ 34 °C) in 45S and more than eleven million people in 85S (relative to the no-savannization) for in-shade environments during the historical period (in which such heat stress conditions did not occur). For instance, these populations would be exposed to a high risk of WBGT (≤34 °C) for at least 1 h/day based on the monthly climatology of the daily maximum values. Of the people impacted
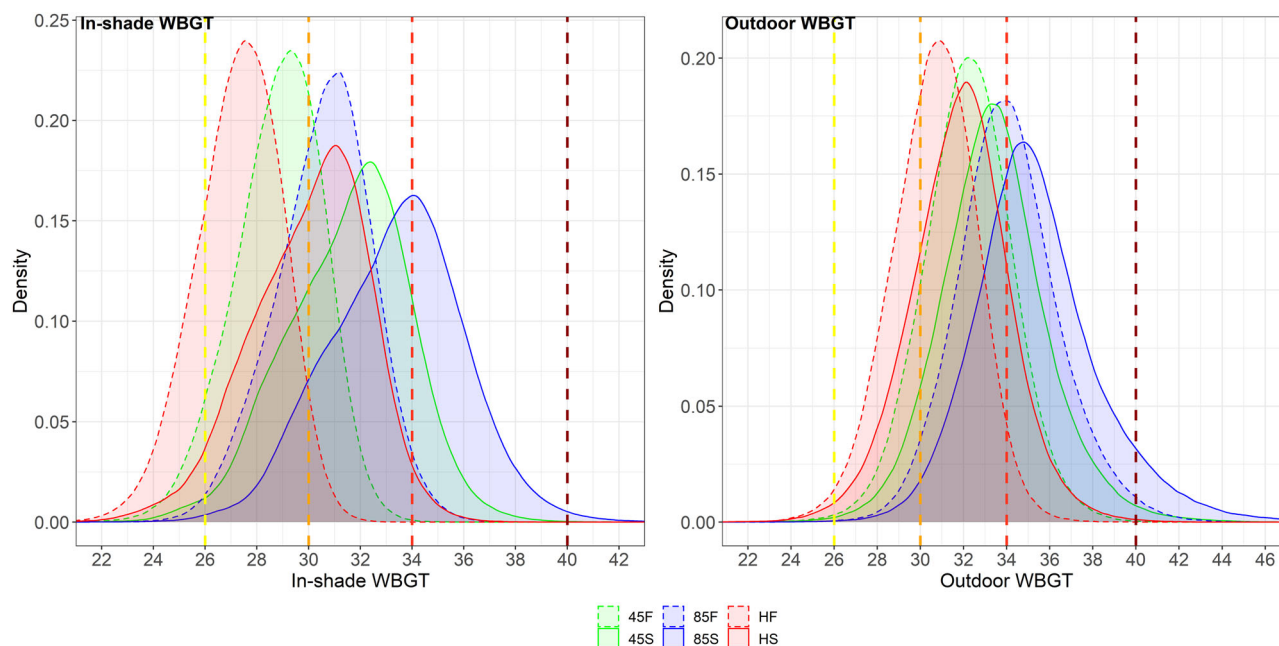

Fig. 2 Distribution of daily maximum in-shadow and outdoor WBGT values (°C). Distribution of daily maximum in-shadow and outdoor WBGT values (°C), according to Amazon rainforest savannization and global climate change scenarios for historical conditions (1980–2010), RCP4.5, and RCP8.5 at the end of the century (2071–2100). Global warming scenarios (Historical – H, RCP4.5 – 45, RCP8.5 – 85) and land-use scenarios (Forested – F and Savannah – S). Risk of heat stress: WBGT ≥ 26 °C and < 30 °C: moderate risk to human health (dashed yellow line); WBGT ≥ 30 °C and <34 °C: high risk to human health (dashed orange line); WBGT ≥ 34 °C: extreme risk to human health (dashed red line); and WBGT ≥ 40 °C: risk to survivability (dashed dark red line).
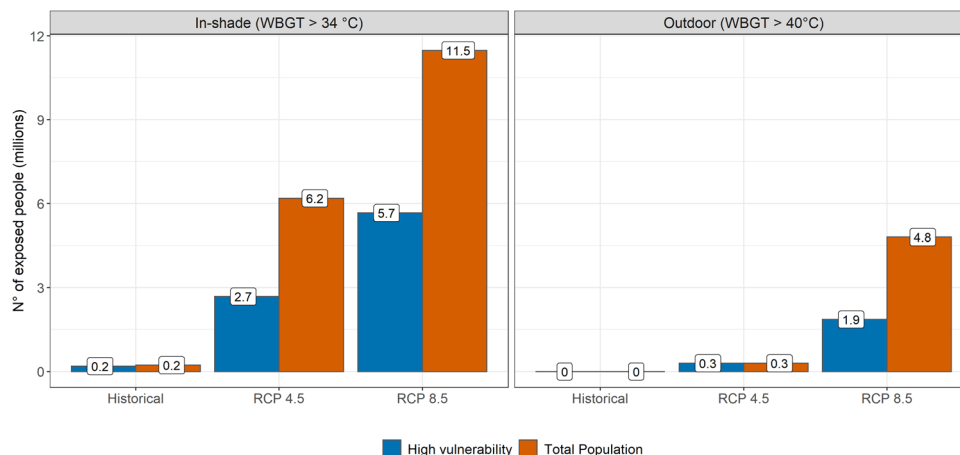
Fig. 3 Combined effects of climate change and deforestation on the number of people under heat stress. Additional numbers of people exposed to heat stress above the extreme risk to human health thresholds due to Amazon rainforest deforestation, according to historical period (1980–2010) and global warming scenarios (2073–2100).

in the RCP8.5 climate change scenario in Brazil, 50% live under conditions of high social vulnerability, with the equivalent of about 5.7 million people exposed (Fig. 3; see in-shade WBGT).

For outdoor conditions and survivability threshold (WBGT > 40 °C), the combined effects of climate change and deforestation could impact a total of five million people by the end of the present century, among whom two million are highly vulnerable. In our estimates, we did not consider population growth or changes in demographic structure, or life expectancy. Thus, these results reflect the isolated effects of climate change and savannization and can be interpreted to represent the effects that would be observed if the current population was exposed to the projected heat stress distributions (Fig. 3; see outdoor WBGT).

The vulnerability of the exposed population was assessed via the Social Vulnerability Index (IVS) of the Brazilian municipalities[31]. This index is based on 16 indicators that reflect fragilities in the health and education system (human capital), urban infrastructure, and income and work[31]. This indicator can be classified as very low or low social vulnerability (SVI less than 0.300), medium social vulnerability (SVI between 0.301 and 0.400), high social vulnerability (SVI between 0.401 and 0.500), and very high social vulnerability (SVI between 0.501 and 1.000)[31].

Of the total of 5565 Brazilian municipalities, 16% (887, inhabited by 30 million people) might be impacted (i.e., increase higher than 0.2 of in-shade WBGT in the hottest month) by the savannization of the Amazon Forest in the RCP8.5 scenario (Fig. 4). Of the impacted population, 42% reside in the northern region of Brazil, which is dominated by municipalities with low population density (with the exception of Manaus, which has a population of more than two million people) and very high social vulnerability. Of the impacted population in the northern region (12 million), 50% live in areas with low resilience and high social vulnerability (IVS ≥ 0.400), reflecting a low capacity to respond and adapt to the combined effects of climate change and deforestation (the impacts of outdoor conditions are presented in the Supplementary Fig. 5).

Conclusions

Based on the results of a numerical climate modeling experiment designed to gauge the effects of Amazon savannization and global climate change scenarios on heat stress, our results suggest that large-scale deforestation of the Amazon rainforest will greatly magnify the risk of exposure to extreme heat associated with climate change on local and regional scales. These heat levels, which will be physiologically intolerable to the human body, will profoundly affect highly vulnerable regions. The heat extreme conditions induced by deforestation could have negative and significantly long-lasting effects on human health, including decreased workability[21,27,28] and increased heat-related morbi-mortality associated with cardiovascular disease[29,30], psychological outcomes[20], and acute kidney diseases[32]. In Brazil, the combined effects of deforestation and climate change are already being reported based on observational data, with the most extreme warming values reported in large deforested areas from 2003 to 2018[33].

Additionally, increased heat stress exposure might impact several areas of the economy via effects on labor productivity, as workers will be exposed to fatal thermal conditions. In Brazil, outdoor workers are already exposed to heat stress, and the projections indicate increasing high-risk exposure over the next decades[34,35]. The 1.5 °C increase in the global average temperature based on the projections of HadGEM2 and GFDL-ESM2M climate models could represent 0.84% of losses in working hours by 2030, the equivalent of 850,000 full-time jobs, especially in the agricultural and construction sectors[36]. Particularly in agriculture, the high risk associated with intense work and thermal overload has already been observed among Brazilian sugarcane cutters[37,38].

In our projections, the combination of land-use change and global warming could further magnify the occupational risks. Moreover, human-induced factors responsible for Amazon savannization, such as increased numbers of forest fires as well as expansion of agricultural areas and mining activities, tend to be characterized by unplanned urbanization, lack of basic sanitary infrastructure, and more frequent informal work[39–41]. These factors link the deforestation process to increased inequality and vulnerability, which act synergistically with the effects of climate change, to further increase the demand for health and social protection services in the Brazilian Amazon region.

The expected effects of heat stress on human health depend on interactions between multiple factors, including the severity and frequency of these events as well as the biological and social vulnerability of the exposed populations. Our results suggest that the deforestation effects on heat stress will most severely affect the Amazon region, which is home to precarious human developments (with respect to health, infrastructure, and income); furthermore, the severity of these effects are enhanced by the limited ability of these regions to respond to the health challenges induced by the combined effects of climate change and deforestation. During the COVID-19 pandemic, the first health
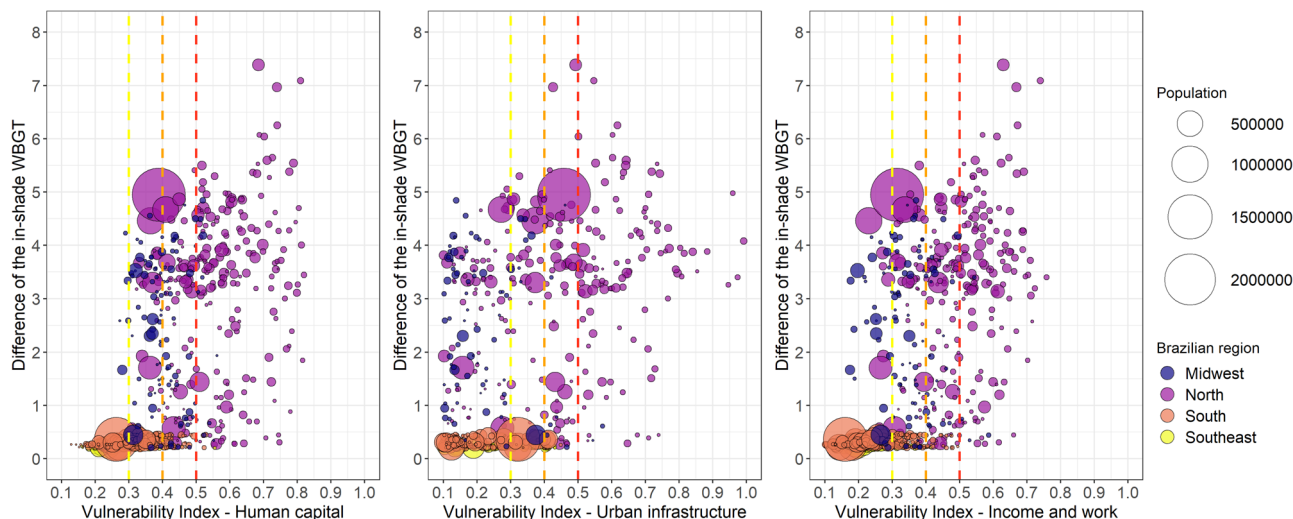
Fig. 4 Municipalities impacted by Amazon savannization RCP8.5 global warming scenario (2073-2100). Municipalities impacted by Amazon savannization RCP8.5 global warming scenario (2073-2100), according to the social vulnerability index (SVI) components. Legend: The impacted municipalities were defined as those with a difference between the average daily maximum of the in-shade WBGT in the hottest month (85S – 85F scenarios) higher than 0.2. The SVI was classified: 0.3-0.4: moderate vulnerability (dashed yellow line); 0.4-0.5: high vulnerability (dashed orange line); greater than 0.5: very high vulnerability (dashed red line). The impacted population comprised 29,648,362 people, of which 42% reside in the northern region, 35% in the southern region, 16% in the southeastern region, and 7% in the midwestern region.

services to collapse in Brazil were in the Amazon region, stressing the synergistic effects of health stressors and the lack of infrastructure in the region.

Finally, our study reveals that the combined effects of Amazon savannization and climate change are significantly associated with threats to human health and well-being, emphasizing the urgent need for coordinated steps to avoid negative effects on vulnerable populations. The local effects of land-use changes are directly linked to forest sustainability policies and strategies, and changes in these areas are within society's reach. In these areas, the health sector could be an important avenue for proposing integrative policies to mitigate risk and vulnerability.

Methods

Meteorological data and WBGT bias correction. The observational data used in this study were from the reanalysis of the European Centre for Medium-Range Weather Forecasts (ECMWF) ERA5[42]. Hourly data fields (i.e., temperature, humidity, solar radiation, and wind speed) were linearly interpolated to match the spatial resolution of the BESM model. Historical period data from 1981 to 2010 was used for the indoor and outdoor environment WBGT calculations and as the current conditions for the bias correction of the model outputs. Observational hourly WBGT values from the reanalysis were used for comparisons with the simulation of the forested Historical period and bias correction procedures. The method used to correct the WBGT bias was based on variable normalization. The standard normal deviate-based scaling used in the experiment is a simple approach that matches only the first and second moments of the observations and model distributions[43]. The correction was applied separately for each time and month to account for possible seasonal and daily cycle changes in the climatological differences. For a given calendar month and time k and a given grid cell i, the scaling parameters are the WBGT (evaluated by 30 years) mean ($Mm_{i,k}$ and $Mo_{i,k}$ for model and observations, respectively) and the standard deviation ($Sm_{i,k}$ and $So_{i,k}$ for model and observations, respectively). For each model WBGT T_i from a particular month and hour (time subscript omitted), the scaled model T_i' is then given by $T_i' = (T_i - Mm_{i,k})So_{i,k}/Sm_{i,k} + Mo_{i,k}$. The means and standard deviations of the forested Historical experiment and the reanalysis were used to correct the computed WBGT bias for the deforestation and RCP experiments. The use of the forested Historic parameters to correct for bias in the deforestation and RCPs experiments is valid as the experimental boundary conditions, although the physics and dynamics of the model were not altered (Supplementary Fig. 6).

Wet-bulb globe temperature estimate. The wet-bulb globe temperature (WBGT) index was calculated for outdoor environments using the method described by Liljegren et al.[44], which considers the effects of temperature, humidity, solar radiation, and wind speed. The in-shade WBGT index was calculated using the method described by Bernard[45], which considers temperature and humidity

and maintains constant wind speed, and excludes the effects of solar radiation. Both methods were recommended by Lemke and Kjellstrom[46] for measuring the effects of climate change on occupational heat stress at the population level. The equations used to calculate the in-shade and outdoor WBGT are given below:

(1) outdoor conditions[44]:

$$WBGT_{outdoor} = 0.7Tnbw + 0.2Tg + 0.1Ta$$

Where $Tnwb$ represents the natural temperature of the wet bulb, Tg is the temperature of the black globe, and Ta is the air temperature. $Tnwb$ and Tg were estimated using air temperature, relative humidity, wind speed, and incident radiation.

(2) in-shade conditions[45]:

$$WBGT_{indoor} = 0.7Tpwb + 0.3Ta$$

Where $Tpwb$ represents the psychrometric wet-bulb temperature

In this study, to describe the spatial distribution of heat stress condition, the daily risks of heat exposure are defined as moderate (WBGT ≥ 26 °C and < 30 °C), high (WBGT ≥ 30 °C and <34 °C), and extreme (WBGT ≥ 34 °C) for work activities (workability), sports, and leisure practices[22]. These tolerance values are similar to the permitted limits of labor scale (work/rest) for intense occupational activities[22] and international sports training[24] in non-cooled places. Under more extreme conditions, exposure to WBGTs greater than 40 °C might compromise survivability in heat-vulnerable groups[2,27].

Population analysis. Bias-corrected WBGT indices were used to calculate indicators of extremes, such as mean daily highs. Thus, from the WBGT hourly data, the maximum daily values were selected, forming a series of 10,266 days for each experiment. From this series, the monthly climatology of the WBGT daily maximums was calculated. The warmest month of this climatology was linearly interpolated for the reference geographic location of the 5565 municipalities in Brazil and related to their populations, according to the number of inhabitants in each municipality as reported for 2019. The vulnerability of Brazilian municipalities and their populations exposed to heat stress conditions was evaluated using the Social Vulnerability Index (SVI)[31]. This index combines 16 indicators to define multiple dimensions of vulnerability, i.e., human capital, urban infrastructure, and income and work, thereby providing a scientific basis for understanding the vulnerability of Brazilian municipalities. Each indicator is represented by a normalized value on a scale that varies between 0 and 1, where 0 corresponds to the ideal or desirable situation. The SVI and its components can be categorized as follows: low or moderate social vulnerability (SVI: < 0.400), high social vulnerability (SVI: 0.401 − 0.500), and very high social vulnerability (SVI: 0.501 − 1.000)[31].

Coupled ocean–atmosphere land ice model. The deforestation and warming scenario simulations were performed using the Brazilian Earth System Model, version 2.5 coupled ocean–atmosphere model (BESM-OA2.5), developed at the Brazilian National Institute for Space Research (INPE). BESM-OA2.5 comprises

the Brazilian Global Atmospheric Model (BAM) of the Center for Weather Forecasting and Climate Studies (CPTEC/INPE) and the Geophysical Fluid Dynamics Laboratory (GFDL) Modular Ocean Model version 4p1 (MOM4p1) of the National Oceanic and Atmospheric Administration (NOAA). More details can be found in Veiga et al.[16] and Capistrano et al.[17]. The BAM atmospheric component, described by Figueroa et al.[47], adopted the horizontal grid resolution truncated at triangular wavenumber 62 (~1.875 × 1.875 degrees of resolution at the Equator) and 28 sigma vertical levels. The surface model SSib[48] was used for heat flux and soil condition calculations. SSib is a static vegetation surface model in which the surface and soil characteristics are seasonally parameterized and spatially distributed using a map with 13 types of earth surface covers. Regional cover type changes in this map allow simulation of changes in surface characteristics, e.g., Amazon basin deforestation.

Experimental design. The numerical experiments were performed with the BESM-OA2.5 using two surface cover boundary conditions: (1) the original SSib vegetation map[49], where the Amazon basin cover corresponds to the biome "Broad-leaf evergreen trees" (tropical rainforest, hereinafter referred to as Forested); and (2) an alternative map in which the Amazon basin region cover is substituted with "Broad-leaf trees with ground cover" (savanna, hereinafter referred to as Deforested). The model simulations follow the CMIP5 experimental design protocol[50]. Three sets of experiments were performed: one Historical run, over the period 1981–2010 (30 years), forced by the observed historical atmospheric equivalent CO_2 concentration (greenhouse gas only), and two global warming scenarios over the period 2071–2100 (30 years), forced by time-dependent changes in greenhouse gas levels projected by the Representative Concentration Pathways 4.5 and 8.5 (RCP4.5 and RCP8.5, respectively)[50]. These three global radiative forcing experimental sets were run with the two surface conditions, i.e., Forested and Deforested Amazon Basin, totaling 6 experiments in all. For all six experiments, 30 years of hourly outputs were processed to calculate the WBGT indices.

Data availability

The data sets that support the findings of this study are available at https://figshare.com/s/a6022896434f1d2ffddd. The inhabitant's number of Brazilian municipalities is open-access data available in https://www.ibge.gov.br/estatisticas/sociais/populacao/9103-estimativas-de-populacao.html?edicao=25272&t=resultados. The data that support the vulnerability analysis of Brazilian municipalities are openly available in http://ivs.ipea.gov.br/index.php/pt/planilha.

Code availability

The code used for calculating the outdoor and in-shade WBGT is open-access produced by A. Casanueva, and it is available on GitHub at the following address: https://rdrr.io/github/anacv/HeatStress/src/R/wbgt.Liljegren.R. The codes of all figures are available at https://figshare.com/s/a6022896434f1d2ffddd.

References

1. Kjellstrom, T., Freyberg, C., Lemke, B., Otto, M. & Briggs, D. Estimating population heat exposure and impacts on working people in conjunction with climate change. *Int. J. Biometeorol.* **62**, 291–306 (2018).
2. Andrews, O., Quéré, C. L., Kjellstrom, T., Lemke, B. & Haines, A. Implications for workability and survivability in populations exposed to extreme heat under climate change: a modelling study. *Lancet Planet. Health* **2**, e540–e547 (2018).
3. Copernicus. *Surface Air Temperature for September.* https://climate.copernicus.eu/surface-air-temperature-september-2020 (2020).
4. INMET. *INMET 7°DISME: Nota metereológica. Onda de Calor Histórica Provoca Recordes De Temperatura Acima Dos 41 ℃ em São Paulo e de 44 ℃ em Mato Grosso do Sul.* https://portal.inmet.gov.br/notasTecnicas (2020).
5. Chou, S. C. et al. Assessment of Climate Change over South America under RCP 4.5 and 8.5 downscaling scenarios. *Am. J. Clim. Change* **03**, 512 (2014).
6. INPE - Instituto Nacional de Pesquisas Espaciais. *Estimativa de Desmatamento por corte raso na Amazônia Legal para 2020 é de 11.088 km².* http://www.obt.inpe.br/OBT/noticias-obt-inpe/estimativa-de-desmatamento-por-corte-raso-na-amazonia-legal-para-2020-e-de-11-088-km2 (2020).
7. Silva Junior, C. H. L. et al. The Brazilian Amazon deforestation rate in 2020 is the greatest of the decade. *Nat. Ecol. Evol.* https://doi.org/10.1038/s41559-020-01368-x (2020).
8. L12187. http://www.planalto.gov.br/ccivil_03/_ato2007-2010/2009/lei/l12187.htm (2009).
9. Albert, J. S. et al. The changing course of the Amazon River in the Neogene: center stage for Neotropical diversification. *Neotrop. Ichthyol.* **16**, e180033 (2018).
10. FAO. *The State of the World's Forests.* www.fao.org. http://www.fao.org/state-of-forests/en/ https://doi.org/10.4060/CA8642EN (2020).
11. Nobre, C. A. et al. Land-use and climate change risks in the Amazon and the need of a novel sustainable development paradigm. *Proc. Natl Acad. Sci. USA* **113**, 10759 (2016).
12. Lovejoy, T. E. & Nobre, C. Amazon tipping point: last chance for action. *Sci. Adv.* **5**, eaba2949 (2019).
13. Nobre, P., Malagutti, M., Urbano, D. F., Almeida, R. A. Fde & Giarolla, E. Amazon deforestation and climate change in a coupled model simulation. *J. Clim.* **22**, 5686–5697 (2009).
14. Coffel, E. D., Horton, R. M. & de Sherbinin, A. Temperature and humidity based projections of a rapid rise in global heat stress exposure during the 21st century. *Environ. Res. Lett.* **13**, 014001 (2018).
15. Nobre, C. A., Marengo, J. A. & Artaxo, P. in *Amazonia Global Change* 145–147. https://doi.org/10.1029/2008GM000716 (2013).
16. Veiga, S. F. et al. The Brazilian Earth System Model ocean–atmosphere (BESM-OA) version 2.5: evaluation of its CMIP5 historical simulation. *Geosci. Model Dev.* **12**, 1613–1642 (2019).
17. Capistrano, V. B. et al. Assessing the performance of climate change simulation results from BESM-OA2.5 compared with a CMIP5 model ensemble. *Geosci. Model Dev.* **13**, 2277–2296 (2020).
18. Kenny, G. P., Yardley, J., Brown, C., Sigal, R. J. & Jay, O. Heat stress in older individuals and patients with common chronic diseases. *CMAJ* **182**, 1053–1060 (2010).
19. Parsons, K. *Human Heat Stress.* (CRC Press, 2019).
20. Tawatsupa, B., Yiengprugsawan, V., Kjellstrom, T., Seubsman, S. & Sleigh, A. Heat stress, health and well-being: findings from a large national cohort of Thai adults. *BMJ Open* **2**, e001396 (2012).
21. Kjellstrom, T., Kovats, R. S., Lloyd, S. J., Holt, T. & Tol, R. S. J. The direct impact of climate change on regional labor productivity. *Arch. Environ. Occup. Health* **64**, 217–227 (2009).
22. ISO 7243. Ergonomics of the thermal environment—assessment of heat stress using the WBGT (Wet Bulb Globe Temperature) Index. *ISO* http://www.iso.org/cms/render/live/en/sites/isoorg/contents/data/standard/06/71/67188.html (2017).
23. Havenith, G. & Fiala, D. Thermal indices and thermophysiological modeling for heat stress. *Compr. Physiol.* **6**, 255–302 (2015).
24. IAAF. *A Practical Guide International Association of Athletics Federations Competition Medical Guidelines, 2013* (2013).
25. Ministério do Trabalho e Emprego (MTE), B. *NR 15 - Atividades e Operações Insalubres: Anexo n° 3 Limites de tolerância para exposição ao calor.* https://www.gov.br/trabalho-e-previdencia/pt-br/composicao/orgaos-especificos/secretaria-de-trabalho/inspecao/seguranca-e-saude-no-trabalho/normas-regulamentadoras/nr-15-anexo-03.pdf (2019).
26. PORTARIA SEPRT N° 1.359, DE 09 DE DEZEMBRO DE 2019. http://www.normaslegais.com.br/legislacao/portaria-seprt-1359-2019.htm (2019).
27. Kjellstrom, T. et al. in *Climate change. A risk assessment* 57–64 (UK Foreign and Commonwealth Office, London, UK, 2015).
28. Spector, J. T., Masuda, Y. J., Wolff, N. H., Calkins, M. & Seixas, N. Heat exposure and occupational injuries: review of the literature and implications. *Curr. Environ. Health Rep.* **6**, 286–296 (2019).
29. Mora, C. et al. Global risk of deadly heat. *Nat. Clim. Change* **7**, 501–506 (2017).
30. de Oliveira, B. F. A. et al. Impacts of heat stress conditions on mortality from respiratory and cardiovascular diseases in Brazil. *Sustain. Debate* **11**, 297–313 (2020).
31. IPEA - Instituto de Pesquisa Econômica Aplicada. IVS: Atlas da Vulnerabilidade Social. http://ivs.ipea.gov.br/index.php/pt/ (2021).
32. Weaver, V. M., Fadrowski, J. J. & Jaar, B. G. Global dimensions of chronic kidney disease of unknown etiology (CKDu): a modern era environmental and/or occupational nephropathy? *BMC Nephrol.* **16**, 145 (2015).
33. Zeppetello, L. R. V. et al. Large scale tropical deforestation drives extreme warming. *Environ. Res. Lett.* **15**, 084012 (2020).
34. Bitencourt, D. P., Alves, L. M., Shibuya, E. K., Cunha, IdeÂda & Souza, J. P. Ede Climate change impacts on heat stress in Brazil—past, present, and future implications for occupational heat exposure. *Int. J. Climatol.* **41**, E2741–E2756 (2021).
35. Bitencourt, D. P., Maia, P. A. & Roscani, R. C. The heat exposure risk to outdoor workers in Brazil. *Arch. Environ. Occup. Health* **75**, 281–288 (2020).
36. ILO - International Labour Office. Working on a warmer planet: the impact of heat stress on labour productivity and decent work (2019).
37. Roscani, R. C., Bitencourt, D. P., Maia, P. A. & Ruas, A. C. Risco de exposição à sobrecarga térmica para trabalhadores da cultura de cana-de-açúcar no Estado de São Paulo, Brasil. *Cad. Saúde Pública* **33**, e00211415 (2017).
38. Bitencourt, D. P., Ruas, Á. C. & Maia, P. A. Análise da contribuição das variáveis meteorológicas no estresse térmico associada à morte de cortadores de cana-de-açúcar. *Cad. Saúde Pública* **28**, 65–74 (2012).
39. Fearnside, P. in *Oxford Research Encyclopedia of Environmental Science* https://oxfordre.com/environmentalscience/view/10.1093/acrefore/

9780199389414.001.0001/acrefore-9780199389414-e-102. https://doi.org/10.1093/acrefore/9780199389414.013.102 (2017).

40. Sonter, L. J. et al. Mining drives extensive deforestation in the Brazilian Amazon. *Nat. Commun.* **8**, 1013 (2017).

41. Ellwanger, J. H. et al. Beyond diversity loss and climate change: Impacts of Amazon deforestation on infectious diseases and public health. *Anais da Academia Brasileira de Ciências* **92**, e20191375 (2020).

42. Hersbach, H. et al. The ERA5 global reanalysis. *Quart. J. R. Meteorol. Soc.* **146**, 1999–2049 (2020).

43. Kumar, S. V. et al. A comparison of methods for a priori bias correction in soil moisture data assimilation. *Water Resour. Res.* **48**, W03515 (2012).

44. Liljegren, J. C., Carhart, R. A., Lawday, P., Tschopp, S. & Sharp, R. Modeling the wet bulb globe temperature using standard meteorological measurements. *J. Occup. Environ. Hyg.* **5**, 645–655 (2008).

45. Bernard, T. E. Prediction of workplace wet bulb global temperature. *Appl. Occup. Environ. Hyg.* **14**, 126–134 (1999).

46. Lemke, B. & Kjellstrom, T. Calculating workplace WBGT from meteorological data: a tool for climate change assessment. *Ind. Health* **50**, 267–278 (2012).

47. Figueroa, S. N. et al. The Brazilian global atmospheric model (BAM): performance for tropical rainfall forecasting and sensitivity to convective scheme and horizontal resolution. *Weather Forecast.* **31**, 1547–1572 (2016).

48. Xue, Y., Sellers, P., Kinter, J. & Shukla, J. A simplified biosphere model for global climate studies. *J. Clim.* **4**, 345–364 (1991).

49. Dorman, J. & Sellers, P. J. A global climatology of albedo, roughness length and stomatal resistance for atmospheric general circulation models as represented by the simple biosphere model (SiB). *J. Appl. Meteorol. Climatol.* **28**, 833–855 (1989).

50. Taylor, K. E., Stouffer, R. J. & Meehl, G. A. An overview of CMIP5 and the experiment design. *Bull. Am. Meteorol. Soc.* **93**, 485–498 (2012).

Author contributions

M.J.B., P.N. and C.A.N. designed the experiments. M.J.B. and P.N. performed experiments/data collection. B.F.A.O., M.J.B. and P.N. analyzed and interpreted the data. M.J.B. and B.F.A.d.O. drafted the paper. P.N. and C.A.N. provided revisions to the scientific content of the manuscript.

Competing interests

The authors declare no competing interests.

Additional information

Supplementary information The online version contains supplementary material available at https://doi.org/10.1038/s43247-021-00275-8.

Correspondence and requests for materials should be addressed to Beatriz Fátima Alves de Oliveira.

Peer review information *Communications Earth & Environment* thanks Daniel Pires Bitencourt and the other, anonymous, reviewer(s) for their contribution to the peer review of this work. Primary Handling Editor: Clare Davis. Peer reviewer reports are available.

Reprints and permission information is available at http://www.nature.com/reprints

Publisher's note Springer Nature remains neutral with regard to jurisdictional claims in published maps and institutional affiliations.